ChemComm

View Online
Dynamic Article Links

Cite this: *Chem. Commun.*, 2011, **47**, 6084–6086

www.rsc.org/chemcomm

COMMUNICATION

Incorporation of graphene in quantum dot sensitized solar cells based on ZnO nanorods†

Jing Chen,[ab] Chu Li,[ac] Goki Eda,[d] Yan Zhang,*[c] Wei Lei,*[a] Manish Chhowalla,[de] William I. Milne[cf] and Wei-Qiao Deng*[b]

Received 10th January 2011, Accepted 30th March 2011
DOI: 10.1039/c1cc10162e

We demonstrate a novel architecture of solar cell by incorporating graphene thin film in a quantum dot sensitized solar cell. Quantum dot sensitized nanorods with a graphene layer exhibited a 54.7% improvement comparing a quantum dot sensitized ZnO nanorods without graphene layer. A fill factor as high as ~62% was also obtained.

Quantum dot sensitized solar cells (QDSSCs) have attracted extensive interest as a means of fabricating highly efficient, low cost photovoltaics.[1] QDs such as CdS,[2] CdSe,[3] and CdTe[4] demonstrate size-dependent band gaps which provide wide-ranging opportunities for harvesting light energy in the visible and infrared regions. This is because these QDs have a large extinction coefficient and upon light absorption, excited electrons can be efficiently transferred to the conduction band of TiO_2[5] or ZnO.[6] In addition, due to the impact ionization effect, it is possible to utilize hot electrons in the QDs to generate multiple electron–hole pairs per photon.[7] Thus, the power conversion efficiency of QDSSCs is expected to exceed the Shockley–Queisser limit (31%).[8]

Despite these features, the efficiencies of QDSSCs based on bare TiO_2 or ZnO film are rather low. The limiting factor is often attributed to the accumulation of electrons in the semiconductor layer due to the relatively slow electron transfer,[9] resulting in the carrier recombination at the semiconductor surface. Thus, suppressing carrier recombination at the semiconductor interface is the key to improving the performance of QDSSCs.

Recently, the discovery of graphene promises a new era of electronics. Graphene has been used in solar cells due to its unique properties. Apart from the transparent electrode,[10,11] graphene can also be used as the electron acceptor layer[10,12] or the hole transport layer[13] in photovolatic devices. In this communication, we first propose and demonstrate the use of a graphene-ZnO composite architecture to enhance the electron transport in QDSSCs. The device in our proposed architecture has been enhanced to almost twice the efficiency of a device without a graphene layer. A fill factor as high as 62% has been obtained, which is one of highest values based on the ZnO nanorod system up to date for QDSSCs.

The fabrication procedure of the graphene-ZnO nanorod is described briefly as follows. Graphene oxide was produced by acid oxidation of natural graphite based on the modified Hummers method.[14,15] GO aqueous suspension with 0.05 mg mL^{-1} was spin-coated on APTES-modified FTO to obtain mono- to few-layer GO thin films. GO was reduced to graphene thin film on FTO/glass in hydrazine vapor at 65 °C overnight.[16] The film thickness was controlled by repeating the spin-coating process multiple times. A ZnO seed layer was deposited on the graphene sheets by ultrasonic spray pyrolysis at 350 °C for 5 min. The substrate was then immersed into a 0.01 M zinc nitrate and 0.01 M hexamethylenetetramine solution and heated at 95 °C for 10 h. After that, the substrate was taken out, washed and dried for sensitizing with CdSe QDs. Oleic acid-capped CdSe QDs were synthesized by a one-pot growth method.[3] The CdSe QDs were loaded on to the ZnO nanorod surface by electrophoretic deposition (ESI).† QDSSCs based on ZnO/CdSe and graphene-ZnO/CdSe photoanodes are labeled as cell A and B, respectively.

Fig. 1(a) shows the absorption spectra of graphene, graphene-ZnO nanorods and graphene-ZnO nanorod/CdSe QD photoanodes. While graphene shows no clear absorption features, ZnO and CdSe exhibit characteristic band edge absorption. It can be seen that the features at 465 and 575 nm appear, indicating the CdSe QDs are adsorbed onto the graphene-ZnO nanorod films. From the excitonic transition peak at 575 nm for graphene-ZnO nanorod/CdSe QD photoanode, the size of these QDs is estimated to be 3.5 nm, based on the analysis reported in the literature.[17]

[a] *School of Electronic Science and Engineering, Southeast University, Nanjing 210096, China. E-mail: lw@seu.edu.cn; Fax: +86-25-83792662; Tel: +86-25-83792650*
[b] *State Key Lab of Molecular Reaction Dynamics, Dalian Institute of Chemical Physics, Chinese Academy of Sciences, Dalian 116023. E-mail: dengwq@dicp.ac.cn; Tel: +86-411 84379571*
[c] *Electrical Engineering Division, Engineering Department, University of Cambridge, 9 JJ Thomson Avenue, Cambridge, CB3 0FA, UK. E-mail: yz236@cam.ac.uk*
[d] *Department of Materials, Imperial College London, Exhibition Road, London, SW7 2AZ, UK*
[e] *Department of Materials Science and Engineering Rutgers University, Piscataway, NJ 08854, USA*
[f] *Department of Information Display, Kyung Hee University, Seoul 130-701, Republic of Korea*

† Electronic supplementary information (ESI) available: Schematic of the fabrication graphene-ZnO nanorod photoanode, FESEM images of ZnO nanorod grown on the different thicknesses of graphene layers, XRD spectra, AFM height images of graphene films with different thicknesses, TEM image of graphene, EDX analysis of ZnO/CdSe, EIS measurement, QDSSCs performance results and photoluminescence decay analysis. See DOI: 10.1039/c1cc10162e

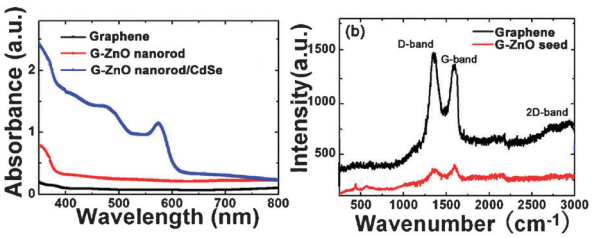

Fig. 1 (a) The absorption spectra of graphene, graphene-ZnO nanorod and graphene-ZnO nanorod/CdSe photoanodes. (b) Raman spectra of graphene and graphene-ZnO seed layer.

Fig. 1(b) shows the Raman spectra for graphene and a graphene-ZnO seed layer. The graphene film exhibits characteristic peaks located at approximately 1598 cm^{-1} and 1350 cm^{-1} (D band), which are assigned to the E_{2g} phonon of sp^2 carbon atoms and the breathing mode of κ-point phonons of A_{1g} symmetry, respectively.[18] After deposition of ZnO seeds onto the graphene sheets, the Raman intensity for the graphene film diminished while the weak characteristic peak of 437 cm^{-1} can be observed, which correspond to the ZnO nonpolar optical photons (E_2) mode.[19]

Fig. 2(a) and (b) show the field-emission scanning electron microscopy (FESEM) images of graphene sheets (thickness of ~9 nm) before and after deposition of ZnO seeds, respectively. The surface of the graphene thin film is highly smooth while the typical wrinkle-like features are weakly visible. After deposition of ZnO seeds, the graphene sheet surface is covered by densely packed and regularly shaped ZnO grains.

Fig. 2(c) and (d) show the FESEM images of ZnO nanorods grown on a monolayer graphene sheet with a diameter of 80–100 nm and a length of 2 μm before and after sensitizing with CdSe QDs, respectively. The graphene-ZnO nanocomposite can be formed by directly depositing ZnO on to the graphene film, because the ZnO is easily entangled and interconnected with graphene during the fabrication.[20,21] The graphene-ZnO composite structure is also verified by XRD spectra (Fig. S3, ESI).† It was found that ZnO nanorod arrays grown on a graphene sheet (thickness ≤ 9 nm) present higher surface ratio than those grown on bare FTO/glass (Fig. S2, ESI).† The performance of QDSSC with thicker graphene would be reduced, caused by severe photocurrent leakage and high loss of spectral transmission through the graphene-ZnO film. An increased amount of QDs can be assembled on ZnO nanorods based on mono- and few-layered graphene sheets due to the enlarged surface area in the engineered graphene-ZnO nanorod architecture. The ZnO nanorods become thicker, developing rough surface features after CdSe QDs loading, indicating high coverage of the CdSe QDs. Fig. 2(e) and (f) show the transmission electron microscopy (TEM) and high-resolution transmission electron microscopy (HRTEM) images of ZnO nanorods with adsorbed CdSe QDs. It can be seen that CdSe QDs with a diameter of ~3.5 nm are uniformly deposited on the ZnO nanorod surface.

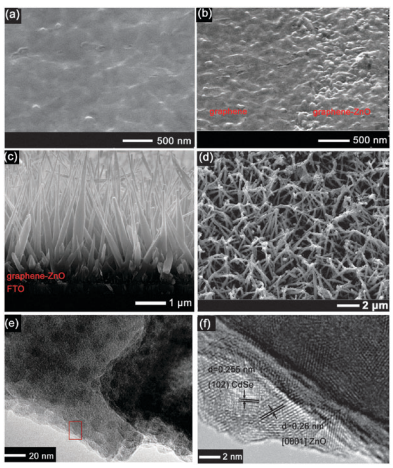

Fig. 2 FESEM image of (a) graphene sheets on FTO/glass. (b) Graphene-ZnO seed layer. (c) Graphene-ZnO nanorod before and (d) after sensitizing with CdSe QD. (e) TEM image of CdSe QDs adsorbed on ZnO nanorods (f) HRTEM image taken from the marked squared region in (e).

Fig. 3(a) shows an energy level schematic diagram of the QDSSC consisting of FTO, graphene, ZnO, CdSe QD and the iodide electrolyte. From the excitonic transition wavelength of 575 nm for the CdSe QDs [Fig. 1(a)], the band gap of the QD is estimated to be around 2.16 eV. The work function of typical graphene is 4.4–4.5 eV.[11,22] Under strong illumination and open circuit conditions, the Fermi-level of ZnO and graphene can be aligned, the band is bent at the interfaces. The offset (~0.2 eV) between the conduction band of ZnO and the work function of graphene is helpful for the reduction of the barrier between ZnO and FTO.[23] It is indicated that the electron transfer from CdSe to the graphene-ZnO nanostructure is energetically favored.

To reveal the influence of graphene film thickness on QDSSC characteristics, we have tested QDSSCs with four different thickness graphene layers [Fig. 3(b)]. The corresponding device characteristics are summarized in Table S1 (ESI).† The best performance of QDSSC was achieved with monolayer graphene sheet. This is attributed to the reduced transmittance of the films and enlarged series resistance arising from the large out-of-plane resistance of graphene thin films, leading to lower short-circuit photocurrent density (J_{sc}) and fill factor (FF).

Fig. 3(c) shows the *I–V* characteristics of cell A and B under simulated 100 mW cm^{-2} irradiation. Cell A exhibited a J_{sc} and FF of 3.37 mA cm^{-2} and 40.9%, respectively, while cell B, which has one monolayer of graphene, exhibited J_{sc} and FF

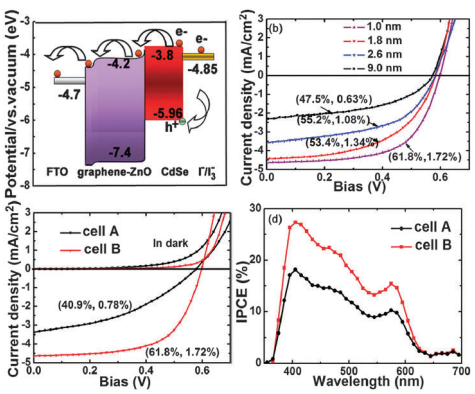

Fig. 3 (a) An energy level schematic diagram for FTO, graphene, ZnO, CdSe QD and electrolyte. (b) *I–V* characteristics of QDSSCs with four different thickness graphene layers (c) *I–V* characteristics of cell A and B. (d) IPCE spectra of cell A and B.

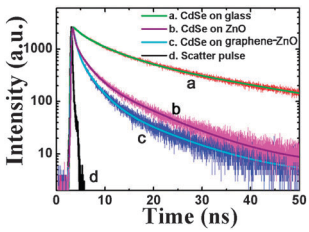

Fig. 4 Emission decay of CdSe QDs deposited on (a) glass (b) ZnO nanorods, (c) graphene-ZnO nanorods. Trace d represents scatter of laser pulse. The excitation wavelength was 467 nm.

of 4.65 mA cm^{-2} and 61.8%, respectively. The FF value obtained in this work is one of the highest values based on the ZnO nanorod system to our knowledge. The improved efficiency with incorporation of a graphene monolayer can be attributed to various factors. The improved J_{sc} can be explained by the higher surface ratio of ZnO nanorods and therefore the higher adsorption sites for CdSe QDs. The FF of a solar cell is determined by two components: shunt resistance (R_{sh}) [$(dV/dI)V = 0$] and series resistance (R_s) [$(dV/dI)V \geq V_{oc}$].[23] It can be seen from Fig. 3(c) that the graphene-ZnO device has smaller R_s than the ZnO device. The R_s for cell A and B can be calculated from the Nyquist plots from Fig. S6 (ESI).† It has been reported that there is a Schottky barrier at the FTO-ZnO electrode, which obstructs electron injection into the electrode, leading to an increased value of R_s.[23] While there is an ohmic contact without a contact barrier between the ZnO nanorod and the graphene film.[21] Therefore, the reduced series resistance between FTO and graphene-ZnO, facilitates the electron transfer and in turn increases the FF. As a result, the overall power conversion efficiency (PCE) is increased by 54.7% to 1.72%. The improved FF indicates that graphene-ZnO architecture helps to reduce charge recombination in QDSSCs.

Fig. 3(d) shows the IPCE of cell A and B, showing a clear spectral response at 575 nm, which corresponds to the first excited state of CdSe QDs. Furthermore, the IPCEs at 575 nm are 15% and 10%, and the maximum IPCEs are 18% and 27% at 400 nm for cell A and B, respectively. These results reflect the higher capability of cell B in converting photons to electrons than cell A, leading to higher photocurrent density, in agreement with the output *I–V* characteristics.

In order to gain insight into the improved device performance, photoluminescence (PL) decay for FTO/ZnO nanorod/CdSe QDs and FTO/graphene-ZnO nanorod/CdSe QDs was measured. Fig. 4 shows the emission decay of CdSe QDs deposited on the FTO and anchored onto ZnO nanorods and graphene-ZnO nanorods, respectively. CdSe QDs directly zdeposited on glass exhibit emission decays with average lifetimes of 10.2 ns. When adsorbed on the ZnO nanorods, their average lifetime was 6.4 ns. CdSe QDs adsorbed on graphene-ZnO nanorod exhibited a lifetime of 4.3 ns. The kinetic parameters of the CdSe emission decay analysis are summarized in Table S2 (ESI).† The electron-transfer rate constants are calculated to be 5.8×10^7 and 1.3×10^8 s^{-1} for the ZnO nanorods and graphene-ZnO nanorods, respectively. The fast decay kinetics observed based on graphene-ZnO architecture is attributed to the reduced resistance between ZnO and FTO, which enhances the electron transfer rate.[24] It is proved to be a quite effective way for capturing photogenerated electrons from CdSe QDs in QDSSC incorporated with the graphene sheets.

In summary, we have demonstrated the use of graphene-ZnO nanorod photoanode is beneficial to enhance the electron transfer in QDSSCs. The reduced series resistance in QDSSC helps to facilitate electron transfer and suppress the interfacial carrier recombination, leading to improvement in FF. These results prompt further detailed studies on the photophysical effects associated with graphene interfaced with inorganic nanostructures.

The authors gratefully thank the financial supports by National Science Foundation of China (No: 50872022, 60801002, 60971017), National Key Basic Research Program 973(2010CB327705), the Chinese 111 project (B07027), the "863" Program of China (2007AA01Z303, 2008AA03A314), NSF Project of Jiangsu province (BK2008319, BK2009264), the "100-Talent Program" of the Chinese Academy of Sciences. Goki Eda would like to acknowledge the Royal Society for the Newton International Fellowship. Manish Chhowalla acknowledges support from the Royal Society through the Wolfson Merit Award.

Notes and references

1 D. R. Baker and P. V. Kamat, *Adv. Funct. Mater.*, 2009, **19**, 805–811.
2 C. H. Chang and Y. L. Lee, *Appl. Phys. Lett.*, 2007, **91**.
3 J. Chen, J. L. Song, X. W. Sun, W. Q. Deng, C. Y. Jiang, W. Lei, J. H. Huang and R. S. Liu, *Appl. Phys. Lett.*, 2009, **94**, 153115.
4 X. F. Gao, H. B. Li, W. T. Sun, Q. Chen, F. Q. Tang and L. M. Peng, *J. Phys. Chem. C*, 2009, **113**, 7531–7535.
5 J. Chen, D. W. Zhao, J. L. Song, X. W. Sun, W. Q. Deng, X. W. Liu and W. Lei, *Electrochem. Commun.*, 2009, **11**, 2265–2267.
6 M. Seol, H. Kim, Y. Tak and K. Yong, *Chem. Commun.*, 2010, **46**, 5521–5523.
7 A. J. Nozik, *Inorg. Chem.*, 2005, **44**, 6893–6899.
8 W. Shockley and H. J. Queisser, *J. Appl. Phys.*, 1961, **32**, 510.
9 I. Robel, V. Subramanian, M. Kuno and P. V. Kamat, *J. Am. Chem. Soc.*, 2006, **128**, 2385–2393.
10 S. R. Sun, L. Gao and Y. Q. Liu, *Appl. Phys. Lett.*, 2010, **96**, 083113.
11 Y. B. Tang, C. S. Lee, J. Xu, Z. T. Liu, Z. H. Chen, Z. B. He, Y. L. Cao, G. D. Yuan, H. S. Song, L. M. Chen, L. B. Luo, H. M. Cheng, W. J. Zhang, I. Bello and S. T. Lee, *ACS Nano*, 2010, **4**, 3482–3488.
12 Z. F. Liu, Q. Liu, Y. Huang, Y. F. Ma, S. G. Yin, X. Y. Zhang, W. Sun and Y. S. Chen, *Adv. Mater.*, 2008, **20**, 3924–3930.
13 S. S. Li, K. H. Tu, C. C. Lin, C. W. Chen and M. Chhowalla, *ACS Nano*, 2010, **4**, 3169–3174.
14 W. S. Hummers and R. E. Offeman, *J. Am. Chem. Soc.*, 1958, **80**, 1339–1339.
15 G. Eda, G. Fanchini and M. Chhowalla, *Nat. Nanotechnol.*, 2008, **3**, 270–274.
16 H. A. Becerril, J. Mao, Z. Liu, R. M. Stoltenberg, Z. Bao and Y. Chen, *ACS Nano*, 2008, **2**, 463–470.
17 W. W. Yu, L. H. Qu, W. Z. Guo and X. G. Peng, *Chem. Mater.*, 2003, **15**, 2854–2860.
18 G. Eda and M. Chhowalla, *Adv. Mater.*, 2010, **22**, 2392–2415.
19 L. Liao, H. B. Lu, J. C. Li, H. He, D. F. Wang, D. J. Fu, C. Liu and W. F. Zhang, *J. Phys. Chem. C*, 2007, **111**, 1900–1903.
20 Y. P. Zhang, H. B. Li, L. K. Pan, T. Lu and Z. Sun, *J. Electroanal. Chem.*, 2009, **634**, 68–71.
21 J. O. Hwang, D. H. Lee, J. Y. Kim, T. H. Han, B. H. Kim, M. Park, K. No and S. O. Kim, *J. Mater. Chem.*, 2011, **21**, 3432–3437.
22 R. Czerw, B. Foley, D. Tekleab, A. Rubio, P. M. Ajayan and D. L. Carroll, *Phys. Rev. B*, 2002, **66**, 033408.
23 A. K. K. Kyaw, X. W. Sun, J. L. Zhao, J. X. Wang, D. W. Zhao, X. F. Wei, X. W. Liu, H. V. Demir and T. Wu, *J. Phys. D: Appl. Phys.*, 2011, **44**, 045102.
24 D. R. Baker and P. V. Kamat, *J. Phys. Chem. C*, 2009, **113**, 17967–17972.